

## Article

# Structural Characterization and Bioactive Compound Evaluation of Fruit and Vegetable Waste for Potential Animal Feed Applications

Miuța Filip <sup>1</sup>, Mihaela Vlassa <sup>1,\*</sup>, Ioan Petean <sup>2</sup>, Ionelia Țăranu <sup>3</sup>, Daniela Marin <sup>3</sup>, Ioana Perhaiță <sup>1</sup>, Doina Prodan <sup>1</sup>, Gheorghe Borodi <sup>4</sup> and Cătălin Dragomir <sup>3</sup>

<sup>1</sup> Raluca Ripan Institute for Research in Chemistry, Babeș-Bolyai University, 30 Fântânele Street, 400294 Cluj-Napoca, Romania; miuta.filip@ubbcluj.ro (M.F.); ioana.perhaita@ubbcluj.ro (I.P.); doina.prodan@ubbcluj.ro (D.P.)

<sup>2</sup> Faculty of Chemistry and Chemical Engineering, Babeș-Bolyai University, 11 Arany Janos Street, 400028 Cluj-Napoca, Romania; ioan.petean@ubbcluj.ro

<sup>3</sup> National Research and Development Institute for Animal Biology and Nutrition-IBNA Balotesti, 1 Calea București Street, 077015 Balotesti, Romania; ionelia.taranu@ibna.ro (I.Ț.); daniela.marin@ibna.ro (D.M.); catalin.dragomir@ibna.ro (C.D.)

<sup>4</sup> National Institute for Research and Development of Isotopic and Molecular Technologies, 65-103 Donath Street, 400293 Cluj-Napoca, Romania; gheorghe.borodi@itim-cj.ro

\* Correspondence: mihaela.vlassa@ubbcluj.ro

**Abstract:** Agricultural waste from the fruit and vegetable industry is used as an alternative source of animal feed, but detailed investigations are required. The aim of this work was to conduct a physico-chemical characterization, through analytical techniques, of fruit and vegetable wastes such as those of golden apples, red apples, carrots, celery, beetroots, and red potato peels. The bioactive compounds in the samples indicated a high carbohydrate content of 50.38 g/100 g in golden apples and 59.38 mg/100 g of organic acids in celery. In addition, the total phenolic content (TPC, mg gallic acid equivalent/g dry weight) varied between 3.72 in celery and 15.51 in beetroots. The antioxidant capacity values were significant. A thermal analysis showed thermal stability and weight loss, underscoring the composition of the solid samples. An infrared spectroscopy (FTIR) analysis showed C-H, O-H, C=O, and N-H functional groups in non-starchy carbohydrates, organic acids, and proteins. Microscopic techniques revealed the microstructure, particle size, and semicrystalline profile of the samples. The ultrastructure (determined via atomic force microscopy (AFM)) of celery consisted of a smooth and uniform surface with a lignin and cellulose texture. These results highlight the importance of fruit and vegetable waste as an alternative source of essential nutrients and bioactive compounds for animal feed.

**Keywords:** fruit and vegetable waste; physico-chemical methods; structural characterization; bioactive compounds



**Citation:** Filip, M.; Vlassa, M.; Petean, I.; Țăranu, I.; Marin, D.; Perhaiță, I.; Prodan, D.; Borodi, G.; Dragomir, C. Structural Characterization and Bioactive Compound Evaluation of Fruit and Vegetable Waste for Potential Animal Feed Applications. *Agriculture* **2024**, *14*, 2038. <https://doi.org/10.3390/agriculture14112038>

Academic Editor: Antonio Natalello

Received: 12 September 2024

Revised: 16 October 2024

Accepted: 26 October 2024

Published: 12 November 2024



**Copyright:** © 2024 by the authors. Licensee MDPI, Basel, Switzerland. This article is an open access article distributed under the terms and conditions of the Creative Commons Attribution (CC BY) license (<https://creativecommons.org/licenses/by/4.0/>).

## 1. Introduction

The waste of fruits and vegetables, obtained after processing in order to obtain food products, contains compounds that are identified in the scientific literature as materials intended for human consumption that are subsequently evacuated, lost, degraded, or contaminated [1]. Agricultural wastes are regarded as a loss of valuable biomass and nutrients, since these wastes have the potential to become useful products or even raw materials for other industries. It is well known that fruits and vegetables are good sources of valuable organic and mineral compounds, along with having high amounts of dietary fiber [2]. In particular, the by-products of the fruit and vegetable industry are of interest, since they are inexpensive and available in large quantities [3]. Agricultural waste (pomace, seeds, peels, stems, pulp, etc.) represents a high percentage of processed fruits and vegetables,

at 20–35% [4]. This fact led to the accumulation of biodegradable matter rich in organic compounds, which can contribute to major environmental pollution through decomposing waste in landfills and the release of harmful gases with greenhouse effects [4,5]. Moreover, the costs to dispose of these agricultural wastes are becoming higher and higher [5]. At present, according to the current EU legislation, a small amount comprising 5–10% of the food waste generated can be used in animal feed [6]. Recent studies considered the characterization of different agricultural by-products in order to use them in the future as animal feed, with the aim of achieving positive effects on animal health and performance, minimizing waste management costs, and avoiding environmental pollution [7]. Moreover, due to the recycling of waste, various food by-products have been included in the catalog of feed materials [8], updated in 2017, through the European Commission regulations [9]. Thus, fruit and vegetable waste could be used as a substitute in animal nutrition and as part of cereal grains and plant protein sources, which would diminish the food competition between humans and animals [10]. In this respect, various fruit and vegetable by-products, which are abundant in bioactive compounds, are used by humans and animals for their nutritional purposes [11].

Carrots (*Daucus carota*) may be processed into juice, concentrates, or dried food [12]. After juicing, approximately 30–50% of the initial mass becomes a by-product of the beverage industry as pulp [13], which provides an inexpensive, sustainable, and renewable source of cellulose, fibers, vitamins, phenolic compounds, and flavonoids [14,15]. Using up to 5% dried carrot processing waste in broiler diets enhances productive performance and economic efficiency [16]. The processing of beetroots (*Beta vulgaris*) results in large amounts of waste materials, including the flesh, crown, and peel [17]. These waste products are being increasingly recognized as a natural source of bioactive compounds with a rich nutritional and commercial value, such as pigments and fibers [18]. The strong antioxidant activity of beetroots is attributed to its content of polyphenolic compounds, and they can be used to stabilize free radicals, preventing the oxidation of biological molecules [19]. In addition, the dietary addition of beetroot waste and carrot waste has been shown to influence the total carotenoid content in the skin and muscle tissues of goldfish (*Carassius auratus*) [20].

Apple (*Malus domestica*) pomace (the pulpy residue remaining after the fruit has been crushed) accounts for ~25% of apples; thus, the remains from the apple juice and cider industry can generate massive amounts of waste. These fruit waste products are a good source of carbohydrates and functionally important bioactive molecules such as proteins, vitamins, minerals, and natural antioxidants [21]. Potatoes (*Solanum tuberosum*) are among the most important agricultural crops that, in order to be consumed, are usually peeled during processing, forming potato peel waste that can vary between 15 and 40% of the initial mass, depending on the peeling method [22]. Potato peels are a by-product rich in starch, non-starchy polysaccharides, lignin, polyphenols, proteins, and small amounts of lipids [23]. In addition, this waste represents a rich material for the extraction of biologically valuable compounds, such as natural antioxidants, dietary fibers, biopolymers, etc. [23]. This waste can be used as an alternative to animal feed due to its natural sources of energy and fiber and its low protein levels [24]. Celery (*Apium graveolens* L.) is rich in vitamins, carotene, protein, cellulose, and other nutrients and is a good source of flavonoids, volatile oil, and antioxidants [25].

For the valorization of agri-food waste, celery root peels were studied by Uzel Aşkın in a case study of raw material [26]. In addition to being a very good source of carbohydrates, celery root peels are a good source of phenolic compounds and pectin, since most of the phenolic components in celery are in the peel [26].

There is growing interest in investigating the potential of by-products as substitutes for conventional feed. These wastes are obtained in significant quantities during the manufacture of agricultural products and by-products that are processed annually in many agricultural countries [6,10].

The aim of the present study was to investigate the physico-chemical and structural properties of some vegetable and fruit wastes to highlight the valuable amounts of essential nutrients and beneficial bioactive compounds contained in these products, which can be exploited as additives in animal feed for the support of animal health.

## 2. Materials and Methods

### 2.1. Sample Preparation

The analytical experiments were carried out in 2023 and 2024. In the current study, fruit waste (golden apples and red apples) and vegetable waste (celery, carrots, beetroots, and red potato peels) were provided by a local food and canning manufacturer from Vâlcea County, Romania (45.04412/24.31295). After the manufacturer obtained juice extractions, the waste of the fruit and vegetable samples (approximately 500 g/sample) was collected in order to be lyophilized for further chemical analyses.

The lyophilization process consisted of two operations: freezing the samples in successive stages and subliming the ice with the help of a higher vacuum. A LyoQuest freeze-dryer (Azbil Telstar, S.L.U., Terrassa, Spain) was used to dry the samples. The residues were placed on lyophilizer shelves. Lyophilization was conducted for 45.5 h in four steps at  $-40\text{ }^{\circ}\text{C}$  and  $-0.5\text{ mbar}$  of pressure. The temperature of the lyophilizer shelves and the sample temperature were measured using temperature sensors.

### 2.2. Chemical Composition

The crude chemical composition was determined according to the WEENDE scheme for the determination of dry matter (DM) ( $103\text{ }^{\circ}\text{C}$ ), crude protein (CP), crude fat (CF), crude cellulose (CC), crude ash (CA), and organic substances. The CC was assessed according to Taranu et al. [27]. The CP in the residues was determined with the semi-automatic classic Kjeldahl method using a Kjeltex auto 1030—Tecator (Tecator AB, Höganas, Sweden) [27]. The ether extract was analyzed using an improved version of the classical continuous solvent extraction method with a Soxhlet extractor, followed by a fat measurement after solvent removal [27]. The DM and CA were determined in accordance with a method from the literature [27]. Neutral detergent fibers (NDFs) were quantified using the Van Soest method reported in [28], and acid detergent fibers (ADFs) were quantified using the Van Soest method reported in [29].

The residue samples were analyzed for their concentration of macro-elements; calcium (Ca) was analyzed according to Anzano et al. [30], and sodium (Na), potassium (K), and magnesium (Mg) were analyzed using atomic absorption spectrometry (AAS) on a Thermo Electron atomic absorption spectrophotometer (Thermo Fisher Scientific Inc., Göteborg, Sweden) [31]. The concentrations of the micro-minerals copper (Cu), iron (Fe), zinc (Zn), and manganese (Mn) were determined using AAS after microwave digestion and mineralization with nitric acid [32]. The working parameters were as follows: wavelength (nm): 324.8 (Cu), 279.5 (Mn), and 213.9 (Zn); bandpass (nm): 0.5 (Cu), 0.2 (Mn), and 0.5 (Zn); lamp current (mA): 5 (Cu), 12 (Mn), and 10 (Zn). The samples were analyzed in triplicate.

### 2.3. HPLC Determination of Carbohydrates, Organic Acids, and Individual Polyphenols

Carbohydrates, organic acids, and phenolic compounds were analyzed using high-performance liquid chromatography (HPLC) on a Jasco chromatograph (Jasco Corporation, Tokyo, Japan) equipped with a UV/Vis detector, a refractive index detector, and an injection valve with a 20  $\mu\text{L}$  sample loop (Rheodyne®, Thermo Fisher Scientific, Waltham, MA, USA). To collect and process the chromatographic data, the ChromPass software (version v1.7, Jasco International Co., Ltd., Tokyo, Japan) was used. The HPLC analyses of carbohydrates were carried out by adapting the method reported in [33]. The determination of organic acids and the analyses of individual phenolic compounds (flavonoids and phenolic acids) were performed according to the methods presented by Filip, M et al. [34,35].

#### 2.4. Analysis of Total Phenolic Content (TPC)

The TPC was measured using the Folin–Ciocalteu colorimetric method with a Specord 205 spectrophotometer (Analytik Jena, GmbH, Berlin, Germany), which was used to detect the blue complex at 760 nm; gallic acid was used as a reference standard [36]. The TPC of each lyophilized compound was quantified as the mg gallic acid equivalent per 100 g of dry weight (mg GAE/100 g). All the determinations were performed in triplicate and the data are presented as the mean  $\pm$  standard deviation (SD).

#### 2.5. Antioxidant Activity

Two different chemical methods, namely DPPH (2,2-diphenyl-1-picrylhydrazyl) and ABTS (2,2'-azino-bis(3-ethylbenzothiazoline-6-sulfonic acid)), were used to evaluate the antioxidant activity of the studied samples.

**DPPH• radical scavenging assay:** A spectrophotometrically modified DPPH method was used to determine the antioxidant activity of the studied samples at 517 nm against methanol as the blank [37]. The free radical scavenging activity of the sample extracts was measured using the absorbance with standard solutions of methanolic Trolox (6-hydroxy-2,5,7,8-tetramethylchroman-2-carboxylic acid). The effective concentrations of DPPH were expressed in  $\mu\text{mol}$  Trolox/100 g dry weight. All the determinations were performed in triplicate and the data are presented as the mean  $\pm$  standard deviation.

**ABTS+• radical scavenging assay:** The antioxidant activity of the samples, determined using the ABTS method, was based on the percentage inhibition of the peroxidation of this radical according to a previously described method [38], with modifications. The ABTS+• radical was generated during a chemical reaction between an ABTS aqueous solution and potassium persulfate [39]. The antioxidant capacity of the studied sample extracts was calculated using a standard curve drawn up for Trolox solutions at 734 nm and expressed as a  $\mu\text{mol}$  Trolox equivalent/100 g dry sample. All the determinations were performed in triplicate and the results are presented as the mean  $\pm$  SD.

#### 2.6. Thermogravimetric Analysis (TGA) and Differential Thermal Analysis (DTG)

The thermal behavior of all the samples was evaluated based on a TG-DTG analysis. The measurements were carried out in the temperature range of 25 to 1200 °C with a heating rate of 10 °C/min, under an inert N<sub>2</sub> atmosphere and at a flow rate of 60 mL/min on a Mettler-Toledo TGA/SDTA851 instrument (Mettler-Toledo, Schwerzenbach, Switzerland).

#### 2.7. Fourier-Transform Infrared Spectroscopy (FTIR) Analysis

An analysis was performed using a Fourier-transform infrared spectrophotometer (FTIR) (Jasco FTIR-610) (Jasco® International Co., Ltd., Tokyo, Japan) equipped with an attenuated total reflectance (ATR) accessory with a horizontal ZnSe crystal (Jasco PRO400S). The samples were placed in direct contact with the ZnSe crystal and then the spectra were recorded at a resolution of 4 cm<sup>-1</sup>. The scans were repeated 100 times.

#### 2.8. X-Ray Diffraction (XRD)

The powder X-ray diffraction patterns were obtained with a Bruker D8 Advance powder diffractometer (Bruker Company, Karlsruhe, Germany) at 40 kV and 40 mA, equipped with an incident beam Ge 111 monochromator using CuK $\alpha$ 1 radiation ( $\lambda = 1.540598 \text{ \AA}$ ). The spectra were scanned at a diffraction angle ( $2\theta$ ) range of 5–80° and a step size of 0.05°/step and 2 s/step. The patterns were indexed using the Dicvol method [40].

#### 2.9. Scanning Electron Microscopy (SEM) Analysis

The analysis was performed on an INSPECT S scanning electron microscope (FEI Company, Hillsboro, OR, USA). The experiment was conducted in a low vacuum at 80 torr, each powder sample was mounted on a stub using carbon tape, and field emissions were performed at 5 kV.

### 2.10. Atomic Force Microscopy (AFM) Analysis

The AFM investigation was effectuated with a JSPM 4210 scanning probe microscope produced by Jeol Company, Tokyo, Japan. The samples were probed in tapping mode using NSC 15 Hard cantilevers produced by MikroMasch Company, Sofia, Bulgaria; they had a resonant frequency of 330 kHz and a force constant of 40 N/m. The topographic images were obtained at a scanning rate of 1–2 Hz, depending on the surface complexity. The images were analyzed with WinSPM 2.0 Processing software, powered by Jeol Company, Tokyo, Japan. The fine microstructural details were observed for a scanned area of 20  $\mu\text{m} \times 20 \mu\text{m}$  and the nanostructural details were observed for an area of 2  $\mu\text{m} \times 2 \mu\text{m}$ . At least three different macroscopic areas were investigated for each sample, and the Ra and Rq surface roughness parameters were measured.

## 3. Results

### 3.1. Chemical Composition

As can be seen from Table 1, there was variation in the DM, with values ranging from 11.85 to 19.30% at a temperature of 65 °C, and between 89.96 and 95.72% at a temperature of 103 °C. The highest CP concentration of all the residues was found for beetroots (16.08%), followed by red potato peels (15.58%).

**Table 1.** The crude chemical composition and fiber content of fruit and vegetable waste.

Chemical Composition (%)	Golden Apples	Red Apples	Carrots	Celery	Beetroots	Red Potato Peels
DM (65 °C)	18.56 $\pm$ 0.17	19.30 $\pm$ 0.16	11.85 $\pm$ 0.11	12.10 $\pm$ 0.12	13.94 $\pm$ 0.14	15.67 $\pm$ 0.14
DM (103 °C)	95.04 $\pm$ 0.13	89.86 $\pm$ 0.19	93.19 $\pm$ 0.15	95.00 $\pm$ 0.11	94.18 $\pm$ 0.11	95.72 $\pm$ 0.11
CP	2.43 $\pm$ 0.09	2.45 $\pm$ 0.06	5.79 $\pm$ 0.06	6.97 $\pm$ 0.08	16.08 $\pm$ 0.07	15.58 $\pm$ 0.08
CF	0.76 $\pm$ 0.04	1.16 $\pm$ 0.03	0.14 $\pm$ 0.015	0.52 $\pm$ 0.03	0.29 $\pm$ 0.02	0.12 $\pm$ 0.01
CA	1.48 $\pm$ 0.07	1.75 $\pm$ 0.08	6.45 $\pm$ 0.08	10.38 $\pm$ 0.17	9.61 $\pm$ 0.07	5.79 $\pm$ 0.08
NDFs	22.42 $\pm$ 0.28	19.85 $\pm$ 0.10	14.19 $\pm$ 0.16	18.85 $\pm$ 0.12	33.15 $\pm$ 0.19	46.29 $\pm$ 0.16
ADF <sub>s</sub>	13.89 $\pm$ 0.16	14.90 $\pm$ 0.15	10.74 $\pm$ 0.18	14.96 $\pm$ 0.16	14.00 $\pm$ 0.26	10.72 $\pm$ 0.22
CC	14.49 $\pm$ 0.15	13.09 $\pm$ 0.13	8.83 $\pm$ 0.12	11.87 $\pm$ 0.23	13.07 $\pm$ 0.16	6.85 $\pm$ 0.24

The values are presented as the mean  $\pm$  standard deviation (SD).

Celery presented the highest amount of CA (10.38%), followed by beetroots (9.61%), carrots (6.45%), and red potato peels (5.79%). Golden apples presented the lowest CA value (1.48%).

Measuring NDFs is the most common method of determining the quantity of fibers for a feed analysis, but they do not represent a unique class of chemical compounds. NDFs include most of the structural components in plant cells (lignin, hemicellulose, and cellulose), but not pectin. Hemicellulose, which is also a carbohydrate present in plant material, is taken into account only when calculating the amount of ADFs. The NDF content varied from the highest amounts, found in red potato peels (46.29%), beetroots (33.15%), and golden apples (22.42%), to the lowest value, which was determined for carrots (14.19%). The samples of celery, red apples, beetroots, and golden apples presented the highest contents of ADFs (14.96, 14.90, 14.00, and 13.89%). With regard to the CC content, golden apples, red apples, and beetroots presented the highest values (14.49–13.97%), while carrots and red potato peels had the smallest values (8.83 and 6.85%).

Concerning the composition of micro- and macro-elements (see Table 2), celery represents a valuable source of Cu (10.480 ppm), Fe (116.400 ppm), Mn (21.190%), and Zn (40.250%), followed by beetroots, with 10.08 ppm of Cu and 33.050% of Zn. Still, red potato peels exhibited the highest concentration of Fe (249.400 ppm). Macro-elements were present in higher quantities in the celery, beetroot, and carrot samples. Thus, the values of K in beetroots (4.502%), celery (4.003%), and red potato peels (3.392%) were followed by the Na values in celery (0.602%), carrots (0.529%), and beetroots (0.367%). Higher values of Ca, P, and Mg were also found in the same vegetables.

**Table 2.** Composition of macro- and micro-minerals.

Waste	Ca	P	Mg	Na	K	Cu	Fe	Mn	Zn
	%	%	%	%	%	ppm	ppm	%	%
Golden apples	0.04 ± 0.002	0.11 ± 0.004	0.06 ± 0.002	0.008 ± 0.0004	0.75 ± 0.037	3.73 ± 0.186	26.09 ± 1.043	6.07 ± 0.303	3.46 ± 0.138
Red apples	0.38 ± 0.019	0.11 ± 0.004	0.105 ± 0.005	0.006 ± 0.0003	1.216 ± 0.061	5.660 ± 0.283	34.910 ± 1.746	5.06 ± 0.253	19.01 ± 0.951
Carrots	0.32 ± 0.013	0.31 ± 0.012	0.117 ± 0.005	0.529 ± 0.021	2.66 ± 0.106	4.16 ± 0.166	25.97 ± 1.039	10.18 ± 0.407	14.60 ± 0.584
Celery	0.48 ± 0.024	0.55 ± 0.028	0.122 ± 0.006	0.602 ± 0.030	4.003 ± 0.200	10.48 ± 0.419	116.40 ± 0.058	21.19 ± 0.848	40.25 ± 2.013
Beetroots	0.12 ± 0.006	0.38 ± 0.019	0.139±	0.367 ± 0.007	4.502 ± 0.225	10.08 ± 0.403	55.65 ± 2.226	16.59 ± 0.664	33.05 ± 1.322
Red potato peels	0.08 ± 0.005	0.33 ± 0.165	0.081 ± 0.004	0.027 ± 0.001	3.392 ± 0.169	8.79 ± 0.439	249.40 ± 9.976	13.66 ± 0.546	21.44 ± 0.858

The values are presented as the mean ± standard deviation (SD).

**3.2. HPLC Determination of Carbohydrates, Organic Acids, and Individual Polyphenols**

The total studied carbohydrates, presented in Figure 1, were found in the largest quantities (g/100 g) for the golden apple samples (50.38) and the carrot samples (46.89).

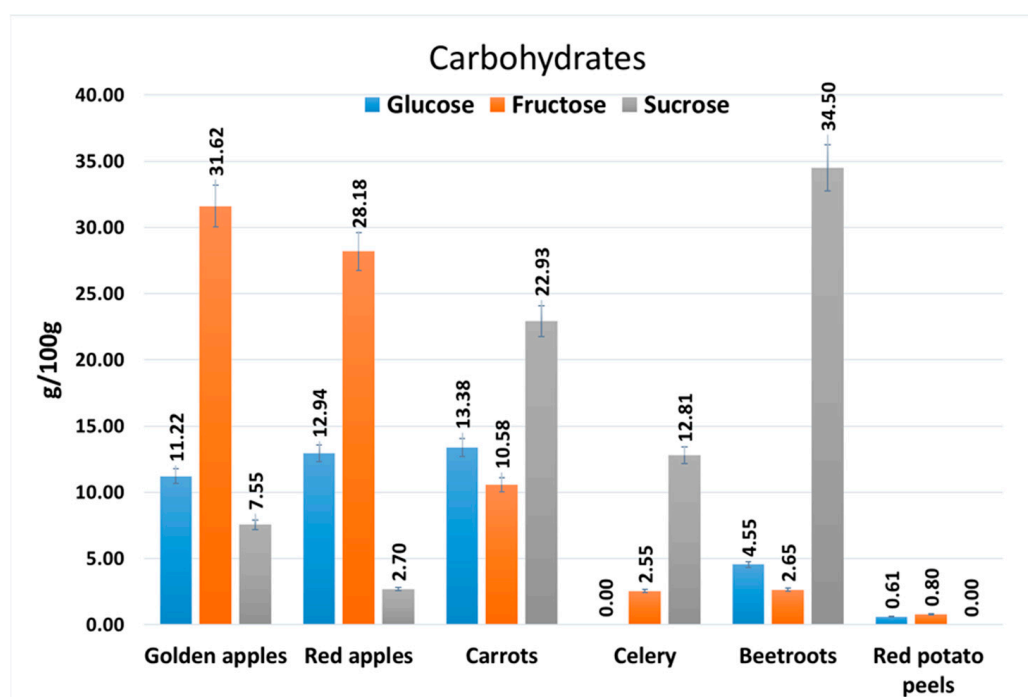


**Figure 1.** The carbohydrate content (mean ± SD) in fruit and vegetable waste.

On the other hand, the smallest value for the total studied carbohydrates was found for red potato peels at 1.41 g/100 g. The celery waste contained 15.35 g/100 g of the studied carbohydrates.

Regarding the organic acid content (Figure 2), the celery and carrot samples had the largest amounts, at 59.38 mg/100 g and 43.81 mg/100 g, respectively. Organic acids were found in relatively important quantities in the golden apple samples, at 35.63 mg/100 g, and the beetroot samples, at 29.96 mg/100 g.

The content of individual flavonoids and phenolic acids had values between 41.44 mg/100 g for the golden apple samples and 129.88 mg/100 g for the beetroot samples. We observed (Figure 3) that the vegetables samples, including those from beetroots, red potato peels, and celery, presented a larger quantity of flavonoids and phenolic acids than the fruit samples from golden and red apples.

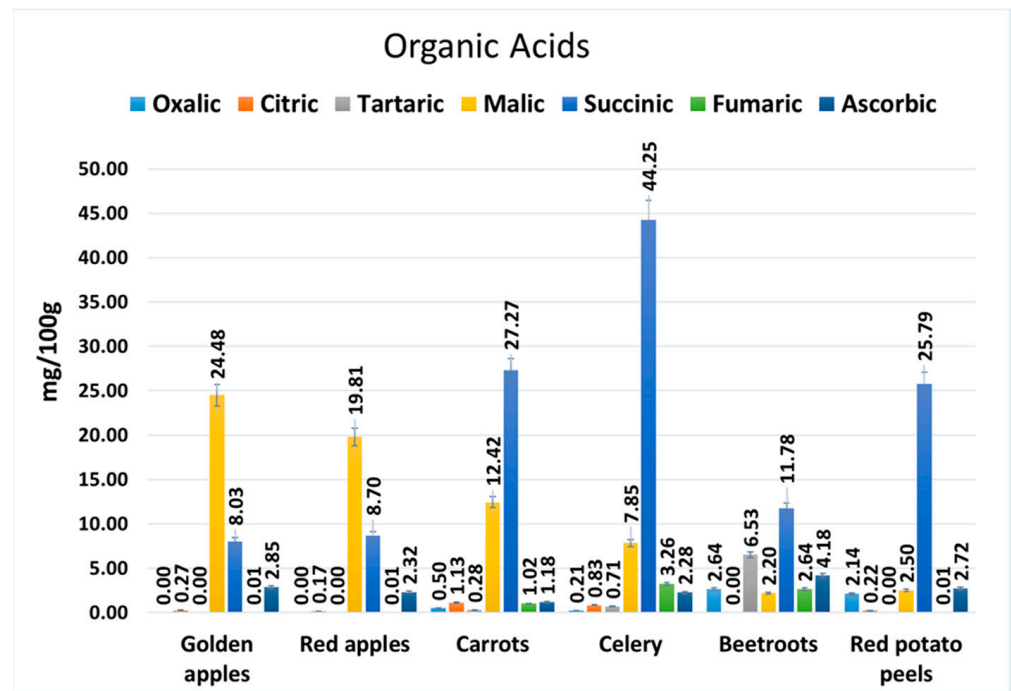


Figure 2. The organic acid content (mean ± SD) in fruit and vegetable waste.

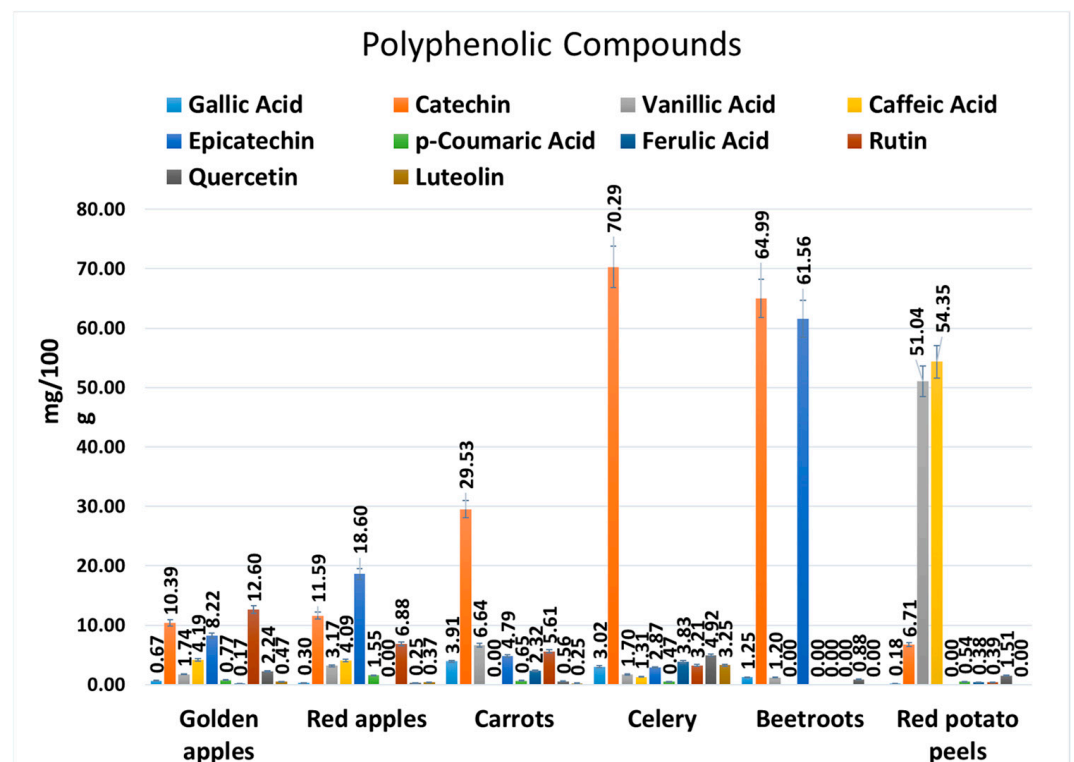


Figure 3. The content of individual polyphenolic compounds (mean ± SD) in fruit and vegetable waste.

### 3.3. Determination of Total Phenolic Content and Antioxidant Capacity

The Total Phenolic Content (TPC) and antioxidant capacity were determined using the DPPH, ABTS, and FRAC radical scavenging activities of methanol extracts of the fruit and vegetable wastes. The results are shown in Table 3.

**Table 3.** Total phenolic content and antioxidant capacity of fruit and vegetable wastes.

	Golden Apples	Red Apples	Carrots	Celery	Beetroots	Red Potato Peels
TPC	6.69 ± 0.03	10.64 ± 0.12	4.69 ± 0.06	3.72 ± 0.02	15.51 ± 0.24	7.75 ± 0.14
DPPH	2066.28 ± 10.63	4075.81 ± 8.49	1438.91 ± 8.13	516.60 ± 4.16	6622.28 ± 35.31	2046.02 ± 13.82
ABTS	1941.81 ± 7.32	3852.48 ± 16.59	1838.29 ± 12.52	1443.91 ± 9.90	7334.98 ± 33.22	3669.92 ± 11.30

TPC, total phenolic content, expressed as gallic acid-equivalent (mg GAE/g dry weight). The DPPH and ABTS assays are expressed as  $\mu\text{mol Trolox}/100\text{ g dry sample}$ . The values are presented as the mean  $\pm$  standard deviation (SD).

The highest TPC (mg GAE/g dry weight) was found for beetroots, at 15.51, followed by red apples, at 10.64, and red potato peels, at 7.75. The TPC in the celery samples was 3.72 mg GAE/g dry weight.

For the apple samples, the determined values (mg GAE/g dry weight) were 6.69 for golden apples and 10.64 for red apples.

In this study, the results of the DPPH and ABTS methods were expressed using the same unit, i.e., Trolox-equivalent antioxidant capacity (micromolar  $\mu\text{mol Trolox}/100\text{ g}$ ), in order to directly compare the results. The highest antioxidant capacity measured with the ABTS assay was found to be 7334.98 for beetroots, followed by 3852.48 for red apples and 3669.92 for red potato peels. For the golden apple, carrot, and celery samples, the amounts found were lower.

Regarding the DPPH antioxidant capacity (micromolar  $\mu\text{mol Trolox}/100\text{ g}$ ), the obtained values followed the same pattern; the highest value was found for beetroots (6622.28), followed by red apples (4075.81). The golden apple and red potato peel samples showed similar values (2066.28 and 2046.02). The lowest value was obtained for celery (516.60).

### 3.4. Thermogravimetric Analysis (TGA) and Differential Thermal Analysis (DTG)

A TGA was performed in order to examine the thermal degradation behavior of the lyophilized selected waste of vegetable and fruit samples, providing important information regarding the pyrolysis process of these materials (Figure 4). As the temperature increased, a mass loss was observed together with the removal of volatile substances.

In a thermodynamic system analysis, heat gain by a system is considered positive, while heat loss is considered negative. The decomposition stages of the powdered fruit and vegetable samples were investigated under a nitrogen atmosphere at temperatures of up to 1200 °C (Figure 4).

In the case of all the freeze-dried samples, the DTA curves showed four stages of thermal decomposition with endothermic effects. Table 4 presents the temperatures and mass losses corresponding to each stage of decomposition and the final residues.

The first stage of decomposition was between 30 and 98.99 °C, and was accompanied by a mass loss of 2.72% for golden apples, 3.85% for red apples, 4.32% for carrots, 4.61% for celery, 4.09% for beetroots, and 5.87% for red potato peels. In this stage, moisture evaporation and a slight weight loss took place due to the loss of light volatiles.

The second stage occurred between 100 and 260 °C, with a mass loss of 37.22% for golden apples, 37.43% for red apples, 39.26% for carrots, 24.17% for celery, and 39.23% for beetroots.

In the third stage of decomposition between 260 and 600 °C, the mass loss, which was equal to 27.89% for carrots and 44.00% for celery, was due to the decomposition of hemicelluloses (220–315 °C), cellulose (315–400 °C), and lignin.

The fourth stage of decomposition, which involved a mass loss of 11.97% for red apples and 25.96% for beetroots, was due to lignin, which decomposes slowly. The total mass losses were in the range of 89.28–96.57% under a nitrogen atmosphere.



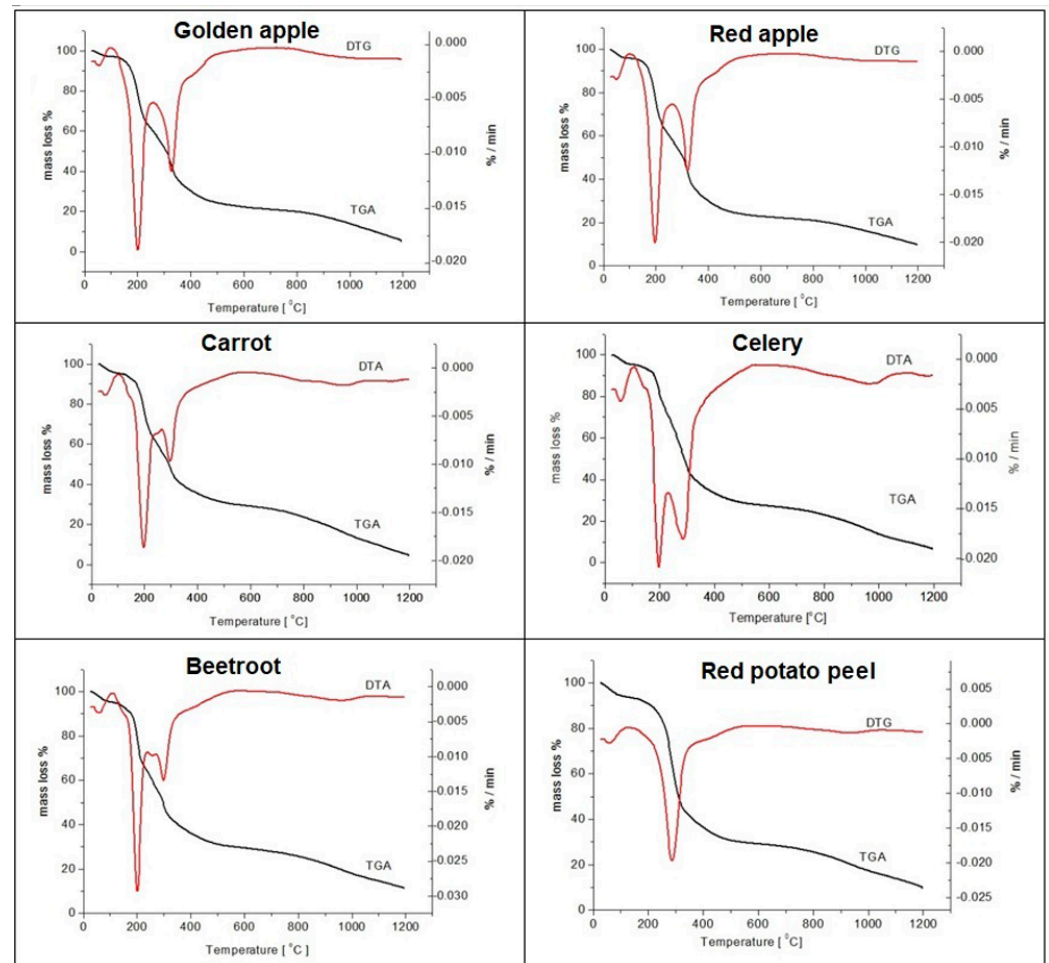


Figure 4. TGA-DTG of the studied fruit and vegetable waste.

Table 4. The stages of thermal decomposition of the studied samples.

Sample	Tmin °C	MI I %	T1 °C	MI II %	T2 °C	MI III %	T3 °C	MI IV %	Tmax °C	TMI %
Golden apples	53.79	2.77	199.93	37.43	328.00	38.91	1189.97	15.22	1200	94.11
Red apples	49.52	3.85	196.1	37.22	321.93	37.09	1144.79	11.97	1200	89.69
Carrots	52.44	4.32	196.96	39.26	295.89	27.28	960.08	24.27	1200	95.64
Celery	57.55	4.61	197.18	24.17	286.38	44.00	962.75	20.43	1200	96.57
Beetroots	56.15	4.09	201.27	39.23	296.91	27.89	919.10	25.96	1200	92.84
Red potato peels	56.76	5.87	-	-	286.43	64.66	928.41	18.79	1200	89.28

Mass loss (MI) stages I, II, III, and IV; TMI, total mass loss.

### 3.5. FTIR-ATR Analysis of Fruit and Vegetable Waste

The FTIR-ATR spectra of the studied golden apple, red apple, carrot, celery, beetroot, and red potato peel samples are shown in Figure 5. Table 5 presents the wavenumbers ( $\text{cm}^{-1}$ ) for each studied sample and the assignment of vibration bands.

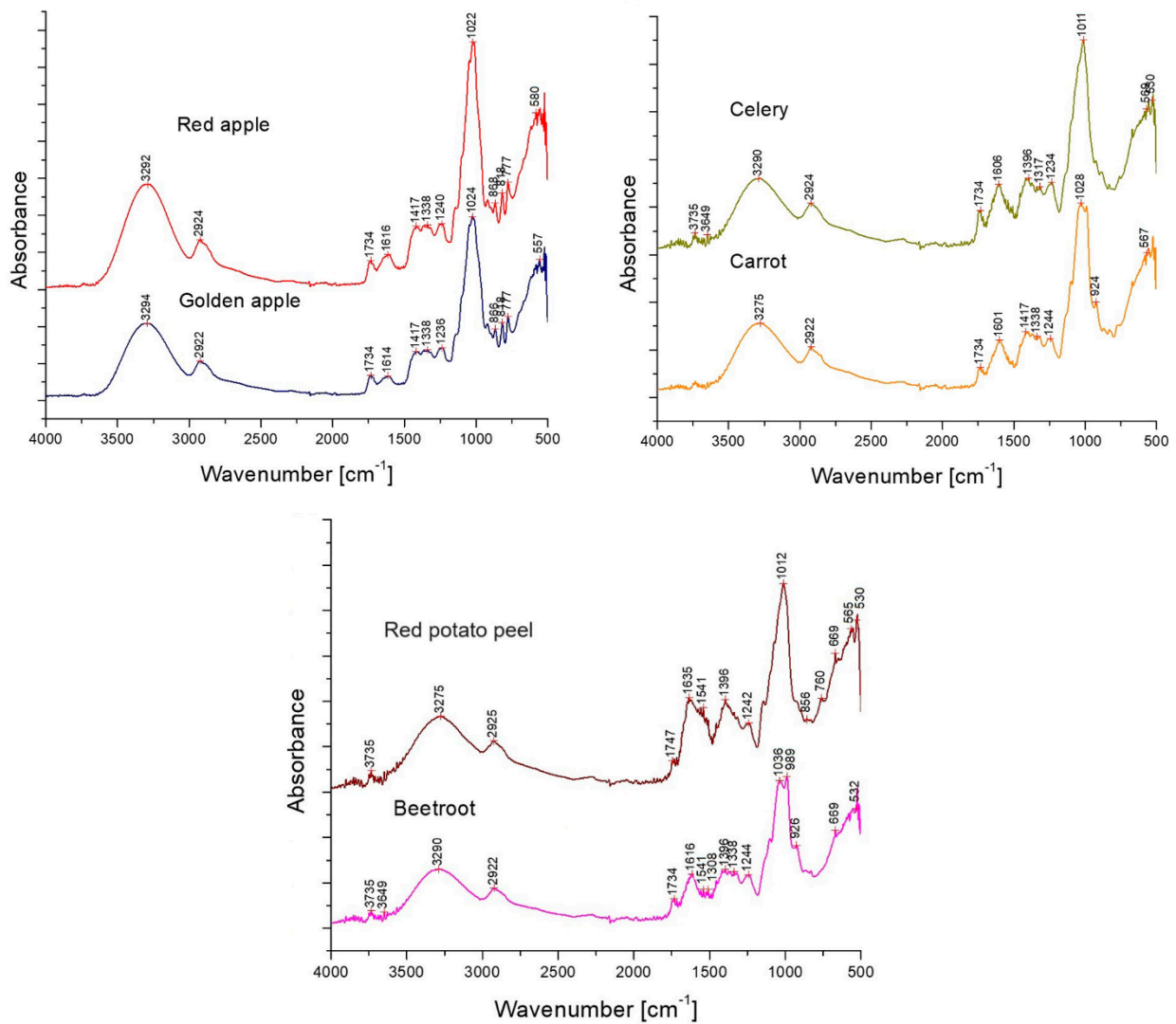


Figure 5. The FTIR-ATR spectra of the studied fruit and vegetable waste.

Table 5. FTIR absorption band assignments.

Golden Apples	Red Apples	Carrots	Celery	Beetroots	Red Potato Peels	Assignment of Vibration Bands	References
-	-	3735	3735; 3649	3735	3735; 3649	O-H group stretching from alcohols, which are abundant in polysaccharides.	[41,42]
3294	3292	3275	3290	3290	3275	O-H group stretching and bending from cellulose or pectins.	[41]
2922	2924	2922	2924	2922	2925	CH <sub>3</sub> , CH <sub>2</sub> , or -CH=CH- aliphatic group asymmetric and symmetric stretching; trans -CH=CH- of beta-carotene and pectins.	[41]
1734	1734	1734	1734	1734	1747	C-O in acetyl group and uranic ester group stretching, or ester groups present in the carboxylic group of ferulic and p-coumaric acids of lignin and/or hemicellulose and pectins.	[41]

Table 5. Cont.

Golden Apples	Red Apples	Carrots	Celery	Beetroots	Red Potato Peels	Assignment of Vibration Bands	References
Wavenumber [ $\text{cm}^{-1}$ ]							
1614	1616	1601	1606	1616	1635	C=O esters from free carboxyl groups (acids); C-O stretching of aryl group present in lignin.	[43]
1417	1417	1417	-	1541	1541	C=C vibration of the aromatic ring.	[44]
1338	1338	1338	1317	1396	1396	CH <sub>3</sub> and CH <sub>2</sub> aliphatic groups.	[44]
1236	1240	1244	1234	1244	1242	C-OH, C-O-C, C-C, C-O, and C=O stretching in sugars, alcohols, and ethers.	[45–47]
1024	1022	1028	1011	1036; 989	1012	C-O bond deformation vibrations in secondary alcohols and aliphatic ethers; C-C, C-OH, C-H ring, and side group vibrations; C-O-C stretching of galacturonic acid, starch, cellulose, and phenols.	[44]
866	868	-	-	926	856	C-O out-of-plane band.	[48]
818–777	818–777	-	-	-	-	C-H, C-C, C-OH, COC, CCO, CCH, and N-H bond deformation and stretching vibrations associated with aromatic rings, carbohydrates, and lignin.	[44]
557	580	567	568	568	565	C-O-O and P-O-C group bending in aromatic phosphates.	[48]

### 3.6. X-Ray Diffraction Analysis

The X-ray diffraction patterns indicated many amorphous compounds and the presence of low organic crystallinity (Figure 6).

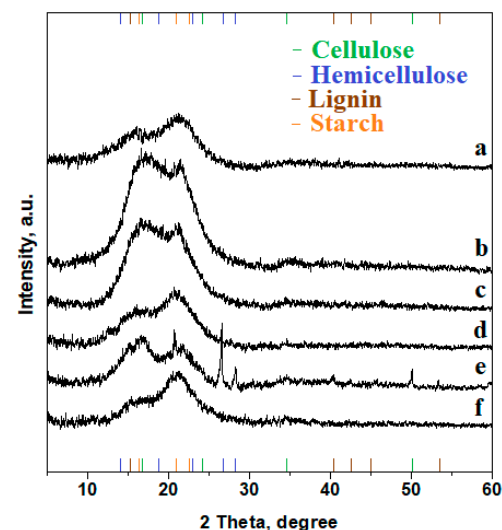
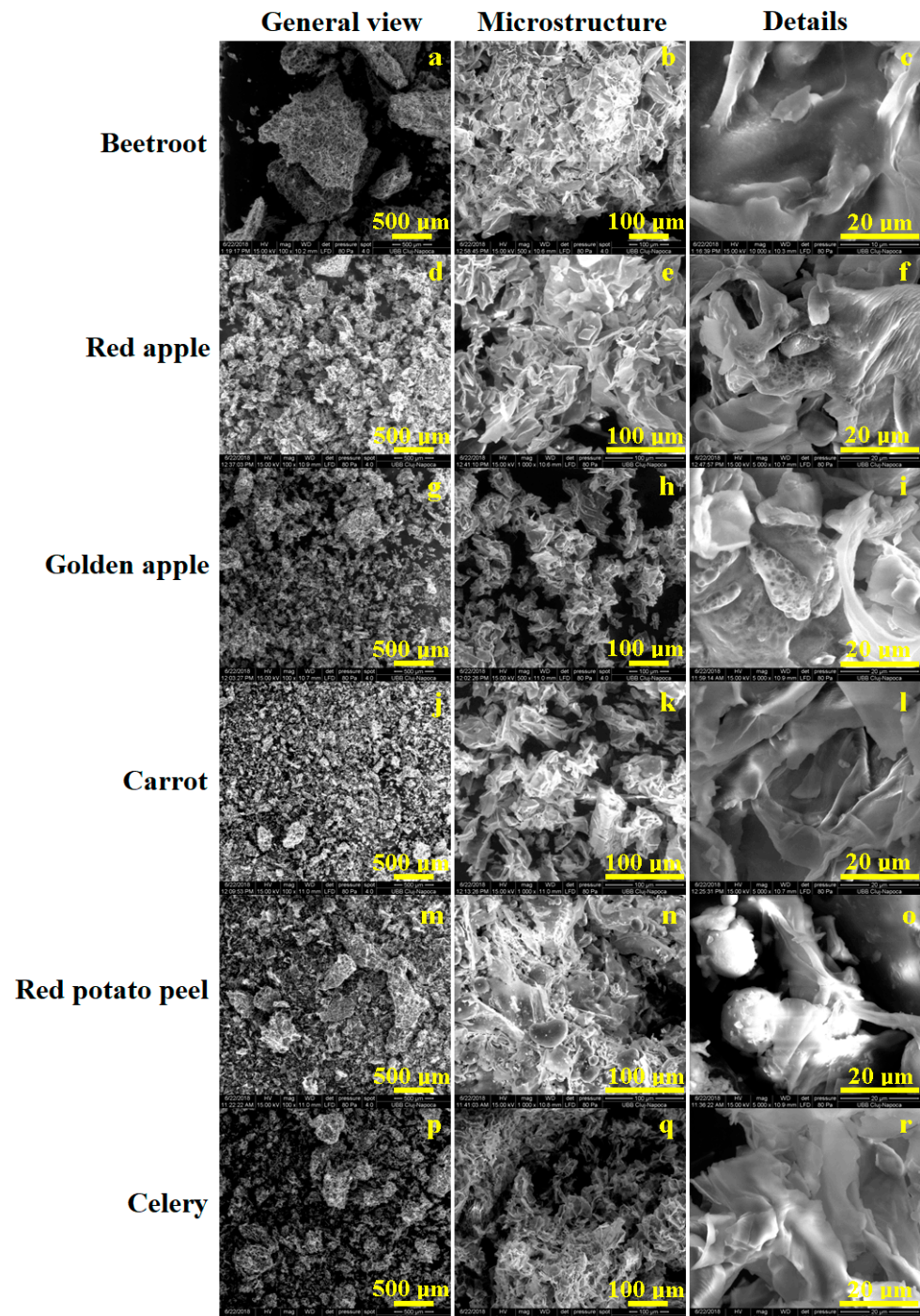


Figure 6. XRD patterns for the wastes of (a) beetroots, (b) red apples, (c) golden apples, (d) carrots, (e) red potato peels, and (f) celery.

The beetroot sample contained starch, hemicellulose, and lignin. In the red apple sample, lignin, cellulose, hemicellulose, and traces of starch were found. The golden apple sample also contained lignin, cellulose, hemicellulose, and traces of starch, and the carrot sample contained starch, cellulose, and lignin. In the red potato peel sample, hemicellulose, starch, cellulose, and lignin were found. The celery sample contained starch, lignin, and cellulose.

### 3.7. SEM Analysis

SEM is a test procedure that scans a sample with an electron beam to produce a magnified image for an analysis. The image contains microscopic information about the surface or near-surface region of a specimen (Figure 7).



**Figure 7.** SEM images of the investigated samples. Beetroot sample at different magnifications: (a)  $\times 100$ , (b)  $\times 500$ , and (c)  $\times 5000$ ; red apple sample at different magnifications: (d)  $\times 100$ , (e)  $\times 1000$ , and (f)  $\times 5000$ ; golden apple sample at different magnifications: (g)  $\times 100$ , (h)  $\times 1000$ , and (i)  $\times 5000$ ; carrot sample at different magnifications: (j)  $\times 100$ , (k)  $\times 1000$ , and (l)  $\times 5000$ ; red potato peel sample at different magnifications: (m)  $\times 100$ , (n)  $\times 1000$ , and (o)  $\times 5000$ ; and celery sample at different magnifications: (p)  $\times 100$ , (q)  $\times 500$ , and (r)  $\times 5000$ .

The beetroot sample presented several conglomerates with irregular shapes of about 700  $\mu\text{m}$ . The microstructural details of the beetroot sample revealed ultrastructural constituents within the flakes.

The apple and carrot powders were very well dispersed, with small particles, while the potato skin and celery samples presented a bimodal aspect, with some clusters of about 350  $\mu\text{m}$ , related mainly to the starch content, surrounded by fine fractions, related to the fiber content. The powders' microstructure revealed a flake-like shape due to the high lignin and cellulose content, giving the powders cohesion and mechanical strength.

The samples from both of the apples revealed a grainy ultrastructural formation (20–40  $\mu\text{m}$  in diameter) of rounded nanoparticles. The details of the carrot sample revealed a lamellar structure, most likely caused by an interlaced texture of lignin and cellulose.

The microstructural detail of the red potato peel sample was heterogeneous due to the presence of starch grains and the lamellar features of hemicellulose interlaced with cellulose and lignin. In the celery sample, there was no evidence of the presence of starch, and well-formed flakes with a fibrous structure were found, induced by lignin and cellulose.

### 3.8. AFM Analysis

The sample particles were further subjected to water dispersion in order to simulate their initial disaggregation during feeding. The dispersions were deposited on glass slides as thin films, naturally dried, and were further investigated with AFM microscopy (Figure 8). The fine microstructural details were observed for a scanned area of 20  $\mu\text{m} \times 20 \mu\text{m}$  and the nanostructural details were observed for an area of 2  $\mu\text{m} \times 2 \mu\text{m}$ . The peel flakes seemed to keep their consistency, but their nanostructural features were enhanced, indicating the possibility of their release into a humid environment. The beetroot sample revealed rounded nanoparticles of about 90 nm, with starch disaggregation due to the wet interactions. These starch nanostructural fractions are more effective in the digestive process, facilitating nutrient absorption. The red and golden apple samples featured a complex ultrastructure based on round nanoparticles of about 35–40 nm that might be related to degraded starch and pectin nanoparticles. The carrot flakes presented a very fine ultrastructure containing fine nanoparticles of about 20 nm that might be related to the presence of beta carotene. The red potato peel ultrastructure showed evidence of starch disaggregation into ultrastructural features consisting of submicron clusters of about 150 nm surrounded by nanoparticles in the range of 60–90 nm. The celery ultrastructure was very interesting, revealing a smooth and uniform surface with a lignin and cellulose texture.

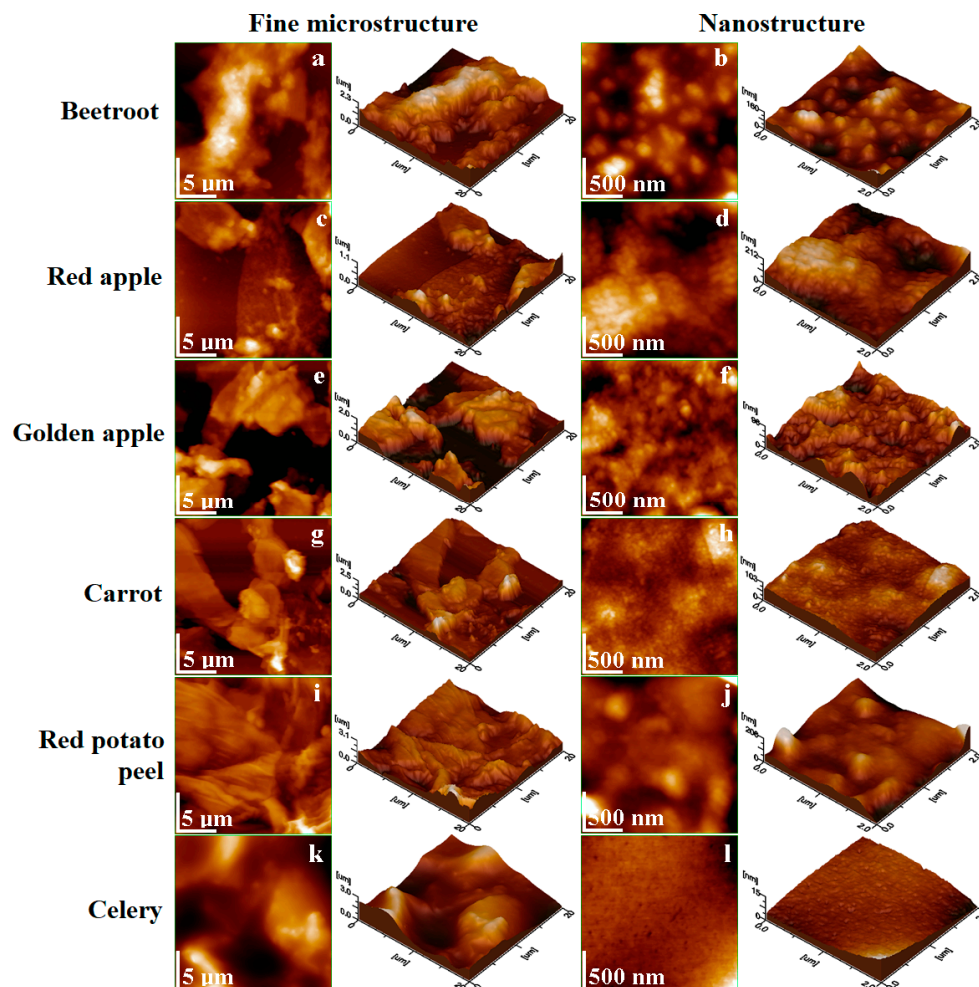


**Figure 8.** AFM topographic images of fruit and vegetable waste: (a) beetroot fine microstructure, (b) beetroot nanostructure, (c) red apple fine microstructure, (d) red apple nanostructure, (e) golden apple fine microstructure, (f) golden apple nanostructure, (g) carrot fine microstructure, (h) carrot nanostructure, (i) red potato peel fine microstructure, (j) red potato peel nanostructure, (k) celery fine microstructure, and (l) celery nanostructure.

#### 4. Discussion

##### 4.1. Evaluation of Chemical Composition and Fiber Content of Fruit and Vegetable Waste

The DM content is an important parameter affecting the storage stability of the powders.

The lyophilization method was selected for analytical purposes only. Another stage of this study will focus on methods for the preservation and use of fruit and vegetable by-products. Many feedstuffs are used in various forms: fresh, ensiled (fermented) using various techniques, or dried using various techniques. The current study focused on the nutritional potential of fresh samples. Thus, the values of the DM for the studied samples ranged from 11.85 to 20.88% at a temperature of 65 °C. The highest protein concentration was found for beetroots (16.08%) and red potato peels (15.58%), with similar values of protein to those presented by other authors for potato peels, at 13.15% [49].

Moreover, the ash content of the samples indicated the mineral quantity. Therefore, a low ash content indicates a low metal content [50]. Celery presented the highest amount of CA (10.38%), and golden apples presented the lowest value (1.48%). Both NDFs and ADFs included cellulose and lignin present in the plant material. The NDF content varied from 46.29% in red potato peels to 14.19% in carrots. The CC content of the studied waste samples was in agreement with the literature data [49,51]. The CC content of the golden

apple, red apple, and beetroot samples presented the highest values, at 14.49 and 13.09 and 13.07%, respectively. Different apple cultivars can influence the physico-chemical composition of apple residues [52]. Moreover, these studied vegetable and fruit wastes are a valuable source of macro- and micro-elements.

#### *4.2. HPLC Determination of the Carbohydrates, Organic Acids, and Individual Polyphenols of Fruit and Vegetable Waste*

The carbohydrate constituents in the studied pomaces are valuable substances due to their positive health effects. The total studied carbohydrates were found in the largest quantities (g/100 g) in the golden apple samples, at 50.38, and the carrot samples, at 46.89. The carbohydrates reported by Luca et al. for carrot pomace represent a rich source of fibers, carbohydrates, and minerals, which suggests its capacity to improve the nutritional value of food products, into which it can be incorporated [53]. The celery waste contained 15.35 g/100 g of the studied carbohydrates, which is within range of literature data on celery waste reporting 5.7–5.9% of the total carbohydrates as sucrose and 33.5–39.3% of the total carbohydrates as mannitol [54].

The studied waste samples are a good source of malic, citric, succinic, and oxalic acids, which behave as antioxidants because they have the ability to chelate metals. The organic acid content in the celery and carrot samples represented the largest amounts, at 59.38 mg/100 g and 43.81 mg/100 g, respectively. In addition, these organic acids enhance appetite; facilitate digestion; and improve potassium, copper, zinc, iron, and calcium absorption [55]. In the fermentation process of rapeseed meal, it was reported that the content of organic acids decreased to varying degrees, while that of succinic acid increased [36].

The content of individual flavonoids and phenolic acids had values between 41.44 mg/100 g in golden apple samples and 129.88 mg/100 g in beetroot samples. The results obtained show that the vegetables waste samples had a larger quantity of flavonoids and phenolic acids than the fruit waste samples.

Javed et al. reported that potato peels are an important source of polyphenols, with their extract comprising protocatechuic acid, caffeic acid, gallic acid, and chlorogenic acid [56]. Some authors reported the content of polyphenols in an aqueous extract of beetroot peels at 70% chlorogenic acid, 21% gallic acid, 6% syringic acid, 2% ferulic acid, and 1% caffeic acid [57].

#### *4.3. Evaluation of Total Polyphenolic Content and Antioxidant Capacity of Fruit and Vegetable Waste*

Waste pomace contains substantial concentrations of polyphenols, which are located mainly in the skin. These valuable active compounds have many health benefits for both animals and humans. In piglets, for example, they improve digestive and fermentative processes [58]. The highest TPC (mg GAE/g dry weight) was found for beetroots at 15.51. The TPC in the celery samples of 3.72 was in agreement with the amounts found in the literature of 3.36–3.50 g GAE/kg [59], 3.3 g GAE/kg [60], and 10.8 g GAE/kg in celery roots [61]. For the apple samples, the determined values (mg GAE/g dry weight) of 6.69 for golden apples and 10.64 for red apples were higher than the values obtained for commercial apple varieties from Croatia, at 2.88–5.72 mg GAE/g dry weight [62]. Some authors reported TPC values in red and purple potatoes of between 7.72 and 40.45 mg GAE/g [63], which are similar to the quantity found in our samples of 7.75 mg GAE/g. The TPC in red-skinned potatoes may be correlated with a high amount of anthocyanins, which are the coloring pigments in red potato varieties [22].

The antioxidant capacities obtained using the DPPH and ABTS assays were expressed in  $\mu\text{mol Trolox}/100\text{ g}$  in order to facilitate a direct comparison of the results. The highest antioxidant capacity measured using the ABTS assay was 7334.98 for beetroots, followed by 3852.48 for red apples and 3669.92 for red potato peels. The scavenging capacity (ABTS assay) of red beetroot varieties was determined by T. Sawicki et al. to be within the range from 37.68 to 49.71  $\mu\text{mol Trolox}/\text{g}$  dry matter; the difference in the antioxidant capacity of

red beetroots depends on the type of root [64]. Regarding the DPPH antioxidant capacity ( $\mu\text{mol Trolox}/100\text{ g}$ ), the obtained values followed the same pattern, with the highest value being found for beetroots (6622.28) and the lowest value being obtained for celery (516.60). W.K. Lau et al. found that the antioxidant capacity of carrots could be significantly reduced through drying or treatment methods [65]. In addition, P.D. Drogoudi et al. showed that the highest antioxidant capacity was found in apple peel tissues and was lower in the flesh tissue, and golden apples showed a lower value in comparison with red apples [66]. The literature findings show that apple and carrot pomaces contain important amounts of bioactive substances with many benefits for both animal and human health. Among these are polyphenols and organic acids, which prevent the multiplication of pathogenic bacteria in the intestine and reduce the diarrhea incidence in piglets after weaning [58]. In addition, polyphenols are recognized as anti-inflammatory compounds. Both apples and carrots, and their by-products, demonstrated antioxidative activity [58]. For example, Sehm et al. (2007) reported a beneficial effect on catalase, glutathione peroxidase, and superoxide dismutase antioxidant enzyme activity by including 3.5% apple pomace in the diet of mice, thus increasing their defense against oxidative stress [67]. The same antioxidant effect was demonstrated for  $\beta$ -carotene, one of the most bioactive compounds found in carrots and their by-products.

Therefore, the obtained results for the studied fruit and vegetable wastes demonstrate that they could be used as bioactive foods due to their strong antioxidant activity.

#### 4.4. Evaluation of Fruit and Vegetable Waste Using TGA and DTG

The TGA provided important information regarding the pyrolysis process of these materials. As the temperature increased, a mass loss was observed together with the removal of volatile substances.

The first stage of decomposition was between 30 and 98.99 °C, and was accompanied by a mass loss of 2.72% for golden apples and 3.85% for red apples. The same results were obtained by Guerrero et al. [68]. A.C. Gowman et al. found a 2% mass loss for apple pomaces under the same conditions [69]. In this stage, moisture evaporation and a slight weight loss took place due to the loss of light volatiles. According to the literature, a weight loss that occurs at 200 °C is related to the beginning of lignin and hemicellulose pyrolysis [70,71]. The second stage occurred with a mass loss between 24.17% for celery and 39.26% for carrots. In the case of potato skins, starch decomposition took place with a distinct peak at 286.43 °C and a mass loss of 64.66% [44]. In the third stage of decomposition (260–600 °C), the mass loss was due to the decomposition of hemicelluloses (220–315 °C), cellulose (315–400 °C), and lignin. The fourth stage of decomposition, which involved a mass loss of 11.97% for red apples and 25.96% for beetroots, was due to lignin, which decomposes slowly over the entire temperature range up to 1200 °C [44,72].

The thermal degradation stages of the fruit and vegetable samples were in agreement with their compositions.

#### 4.5. Evaluation of Fruit and Vegetable Waste Using ATR-FTIR

The FTIR analysis provided data on the absorption regions of the characteristic groups, along with a rapid process for interpreting these data [42].

The FTIR-ATR spectra of the samples showed intense bands at 3294–3292  $\text{cm}^{-1}$ , corresponding to O-H group stretching and bending from cellulose or pectins, and at 2922–2924  $\text{cm}^{-1}$ , corresponding to  $\text{CH}_3$ ,  $\text{CH}_2$ , or  $-\text{CH}=\text{CH}-$  aliphatic group asymmetric and symmetric stretching, as well as the  $\text{trans-CH}=\text{CH}-$  of beta-carotene and pectins [41,42]. The bands at 1734  $\text{cm}^{-1}$  resulted from C=O, the most widespread group in hemicellulose and pectin [41]. The absorption at 1614–1616  $\text{cm}^{-1}$  was attributed to C=O groups from esters from the free carboxyl groups (acids) and/or C-O stretching of the aryl groups present in lignin [43]. The band detected at 1635  $\text{cm}^{-1}$  was assigned to the C=N vibration group in the potato spectra. A closer examination of the spectra revealed the presence of a band at 1541  $\text{cm}^{-1}$ , which was characteristic of the deformation of the C-H bond vibration and C=C



vibration of the aromatic ring [44]. The region of the ATR-FTIR spectra between 800 and 1300  $\text{cm}^{-1}$  was considered to be the specific region for carbohydrates, which allowed for the identification of the major characteristic chemical groups for certain polysaccharides [45]. The most intense peak, with a maximum in the area of 1024–1022  $\text{cm}^{-1}$ , belonged to the C-O deformation vibration bonds in secondary alcohols and aliphatic ethers; the C-C, C-OH, C-H ring, and side group vibrations of cellulose and hemicellulose; and the C-O-C stretching of galacturonic acid [46,47]. The bands between 1065 and 989  $\text{cm}^{-1}$  corresponded to -C-C, -C-OH, and -C-H group vibrations from cellulose and phenols [48].

#### 4.6. Evaluation of Fruit and Vegetable Waste Using X-Ray Diffraction, SEM, and AFM

The observed patterns indicated many amorphous compounds, with the decomposition of cellulose indicating an amorphous carbon structure with randomly oriented aromatic carbon sheets and a low organic crystallinity [73]. Microscopic information about the surface or near-surface region showed that the fruit and vegetable waste contained starch, cellulose, hemicellulose, and lignin [74].

The surface SEM morphology analysis of the fruit and vegetable waste revealed differently shaped particles with an agglomerated cluster-like morphology. The microstructure of the powders revealed a flake-like shape due to the high lignin and cellulose contents, giving them cohesion and mechanical strength. According to Anukriti et al., a morphology and surface analysis of solar-dried vegetables through XRD and SEM showed the effect of solar drying on the nutritional value of green leafy vegetables [74]. The structure of the celery leaves was dense and uniform, without any detectable gel breaks, and the pores were smaller and fewer [75].

The fine microstructural information revealed using AFM is in good agreement with the SEM observations of the microstructure details. The peel flakes seemed to maintain their consistency, but their nanostructural features were enhanced, indicating the possibility of their release into a humid environment. Ultrastructure AFM provides images with a near-atomic resolution for measuring the surface topography of dried fruits and vegetables, revealing their surfaces and textures. These are properties that influence the behavior of these wastes as an animal feed additive. In the literature, AFM analyses have been used to clarify the influences of blanching treatments on carrot texture [76].

## 5. Conclusions

The abundance of the biologically active substances in vegetable and fruit waste potentially makes these residues valuable products for the livestock industry. The results obtained show that the CP content in the beetroots and red potato peels was between 16.08 and 15.58%. The CA content was higher in the celery samples, at 10.38%, and the NDF and ADF content was 18.85 and 14.96%, respectively. All the samples contained fibers in the form of lignin, cellulose, hemicellulose, starch, and pectin. The highest values of macro- and micro-elements in celery included Zn at 40.250%, Mn at 21.190%, and Cu at 10.480 ppm. In addition, the beetroot samples contained 4.502% K, and the red potato peel samples contained 249.400 ppm, representing the highest Fe content of all the samples.

The total studied carbohydrates were found in the largest quantities (g/100 g) in the golden apple samples at 50.38, followed by the carrot samples at 46.89. The celery samples contained 15.35 g/100 g of the studied carbohydrates. Regarding the organic acid content, the celery and carrot samples had the largest amounts, at 59.38 mg/100 g and 43.81 mg/100 g, respectively. The content of individual flavonoids and phenolic acids was between 41.44 mg/100 g (for the golden apple samples) and 129.88 mg/100 g (for the beetroot samples). The vegetable samples, including from beetroots, red potato peels, and celery, presented a larger quantity of flavonoids and phenolic acids than the fruit samples, which included golden and red apples.

The highest TPC (mg GAE/g dry weight) was found for beetroots at 15.51, followed by red apples at 10.64, and red potato peels at 7.75. The highest antioxidant capacities (micromolar  $\mu\text{mol}$  Trolox/100 g), as measured using the ABTS assay, were found in beetroots

at 7334.98; in red apples at 3852.48; and in red potato peels at 3669.92. Regarding the DPPH antioxidant capacity, the obtained values (micromolar  $\mu\text{mol}$  Trolox/100 g) were the highest for the beetroot (6622.28) and red apple (4075.81) samples.

TGA-DTG analysis was used to determine the thermal stability and weight loss, which confirmed the composition of the solid samples. FTIR analysis showed the presence of C-H, O-H, C=O, and N-H functional groups in non-starchy carbohydrates, organic acids, and proteins. The SEM and XRD microstructural analyses revealed the particle size and the semicrystalline profile of the samples. The AFM ultrastructure of celery consisted of a smooth and uniform surface with a lignin and cellulose texture.

These results indicate the importance of fruit and vegetable waste as an alternative source of essential nutrients and bioactive compounds for livestock feeds.

**Author Contributions:** Conceptualization, M.V. and M.F.; methodology, M.F., M.V., I.P. (Ioan Petean), D.M., I.P. (Ioana Perhaiță), D.P. and G.B.; software, M.F., I.T. and C.D.; validation, M.F., I.P. (Ioan Petean) and D.P.; formal analysis, I.P. (Ioan Petean), D.M., I.P. (Ioana Perhaiță), D.P. and G.B.; investigation, M.F., M.V., I.P. (Ioan Petean), D.M., I.P. (Ioana Perhaiță), D.P. and G.B.; resources, M.V. and C.D.; data curation, I.T., D.M. and C.D.; writing—original draft preparation, M.V. and M.F.; writing—review and editing, M.V. and C.D.; visualization, I.T.; supervision, I.T. and M.V.; project administration, M.V.; funding acquisition, C.D. All authors have read and agreed to the published version of the manuscript.

**Funding:** This research was funded by the Romanian Ministry of Research, Innovation and Digitization under grant No. PN2320-0201.

**Institutional Review Board Statement:** Not applicable.

**Data Availability Statement:** The data are contained within the article.

**Conflicts of Interest:** The authors declare no conflicts of interest.

## References

- Giroto, F.; Alibardi, L.; Cossu, R. Food Waste Generation and Industrial Uses: A Review. *Waste Manag.* **2015**, *45*, 32–41. [CrossRef] [PubMed]
- Esparza, I.; Jiménez-Moreno, N.; Bimbela, F.; Ancín-Azpilicueta, C.; Gandía, L.M. Fruit and Vegetable Waste Management: Conventional and Emerging Approaches. *J. Environ. Manag.* **2020**, *265*, 110510. [CrossRef] [PubMed]
- Lau, K.Q.; Sabran, M.R.; Shafie, S.R. Utilization of Vegetable and Fruit By-Products as Functional Ingredient and Food. *Front. Nutr.* **2021**, *8*, 661693. [CrossRef] [PubMed]
- Pathania, S.; Kaur, N. Utilization of Fruits and Vegetable By-Products for Isolation of Dietary Fibres and Its Potential Application as Functional Ingredients. *Bioact. Carbohydr. Diet. Fibre* **2022**, *27*, 100295. [CrossRef]
- Sagar, N.A.; Pareek, S.; Sharma, S.; Yahia, E.M.; Lobo, M.G. Fruit and Vegetable Waste: Bioactive Compounds, Their Extraction, and Possible Utilization. *Compr. Rev. Food Sci. Food Saf.* **2018**, *17*, 512–531. [CrossRef]
- Shurson, G.C.; Dierenfeld, E.S.; Dou, Z. Rules are meant to be broken—Rethinking the regulations on the use of food waste as animal feed. *Resour. Conserv. Recycl.* **2023**, *199*, 107273–107283. [CrossRef]
- Ajila, C.M.; Brar, S.K.; Verma, M.; Tyagi, R.D.; Godbout, S.; Valéro, J.R. Bio-Processing of Agro-Byproducts to Animal Feed. *Crit. Rev. Biotechnol.* **2012**, *32*, 382–400. [CrossRef]
- European Commission. COMMISSION REGULATION (EU) No 68/2013 of 16 January 2013 on the Catalogue of feed materials. *Off. J. Eur. Union* **2013**, *29*, 1–64. Available online: <https://eur-lex.europa.eu/LexUriServ/LexUriServ.do?uri=OJ:L:2013:029:0001:0064:EN:PDF> (accessed on 15 July 2024).
- European Commission. COMMISSION REGULATION (EU) 2017/1017 of 15 June 2017 amending Regulation (EU) No 68/2013 on the Catalogue of feed materials. *Off. J. Eur. Union* **2017**, *159*, 48–119. Available online: <https://eur-lex.europa.eu/legal-content/EN/TXT/PDF/?uri=CELEX:32017R1017> (accessed on 15 July 2024).
- Georganas, A.; Giamouri, E.; Pappas, A.C.; Papadomichelakis, G.; Galliou, F.; Manios, T.; Tsiplakou, E.; Fegeros, K.; Zervas, G. Bioactive Compounds in Food Waste: A Review on the Transformation of Food Waste to Animal Feed. *Foods* **2020**, *9*, 291. [CrossRef]
- Lee, K.; Malerba, F. Catch-up Cycles and Changes in Industrial Leadership: Windows of Opportunity and Responses of Firms and Countries in the Evolution of Sectoral Systems. *Res. Policy* **2017**, *46*, 338–351. [CrossRef]
- Sharma, K.D.; Karki, S.; Thakur, N.S.; Attri, S. Chemical Composition, Functional Properties and Processing of Carrot—A Review. *J. Food Sci. Technol.* **2012**, *49*, 22–32. [CrossRef] [PubMed]
- Bao, B.; Chang, K.C. Carrot Pulp Chemical Composition, Color, and Water-holding Capacity as Affected by Blanching. *J. Food Sci.* **1994**, *59*, 1159–1161. [CrossRef]

14. Shyamala, B.N.; Jamuna, P. Nutritional Content and Antioxidant Properties of Pulp Waste from *Daucus carota* and *Beta vulgaris*. *Malays. J. Nutr.* **2010**, *16*, 397–408. [PubMed]
15. Ikram, A.; Rasheed, A.; Ahmad Khan, A.; Khan, R.; Ahmad, M.; Bashir, R.; Hassan Mohamed, M. Exploring the Health Benefits and Utility of Carrots and Carrot Pomace: A Systematic Review. *Int. J. Food Prop.* **2024**, *27*, 180–193. [CrossRef]
16. Hashem, N. The Use of Dried Carrot Processing Waste in Broiler Diets. *J. Anim. Poult. Prod.* **2012**, *3*, 423–435. [CrossRef]
17. Vulić, J.J.; Čebović, T.N.; Čanadanović-Brunet, J.M.; Četković, G.S.; Čanadanović, V.M.; Djilas, S.M.; Tumbas Šaponjac, V.T. In Vivo and in Vitro Antioxidant Effects of Beetroot Pomace Extracts. *J. Funct. Foods* **2014**, *6*, 168–175. [CrossRef]
18. Costa, A.P.D.; Hermes, V.S.; Rios, A.O.; Flôres, S.H. Minimally Processed Beetroot Waste as an Alternative Source to Obtain Functional Ingredients. *J. Food Sci. Technol.* **2017**, *54*, 2050–2058. [CrossRef]
19. Singh, A.; Ganesapillai, M.; Gnanasundaram, N. Optimizat on of Extraction of Betalain Pigments from *Beta vulgaris* Peels by Microwave Pretreatment. *IOP Conf. Ser. Mater. Sci. Eng.* **2017**, *263*, 032004. [CrossRef]
20. Jasmin, K.J.; Somanath, B. Carrot Waste and Beetroot Waste Supplemented Diet Promoting Carotenoid Changes in Freshwater Goldfish *C. auratus*. *Int. J. Life Sci. Res.* **2016**, *4*, 105–113.
21. Egüés, I.; Hernandez-Ramos, F.; Rivilla, I.; Labidi, J. Optimization of Ultrasound Assisted Extraction of Bioactive Compounds from Apple Pomace. *Molecules* **2021**, *26*, 3783. [CrossRef] [PubMed]
22. Sepelev, I.; Galoburda, R. Industrial Potato Peel Waste Application in Food Production: A Review. *Res. Rural Dev.* **2015**, *1*, 130–136.
23. Wu, Z.G.; Xu, H.Y.; Ma, Q.; Cao, Y.; Ma, J.N.; Ma, C.M. Isolation, Identification and Quantification of Unsaturated Fatty Acids, Amides, Phenolic Compounds and Glycoalkaloids from Potato Peel. *Food Chem.* **2012**, *135*, 2425–2429. [CrossRef] [PubMed]
24. Ncobela, C.N.; Kanengoni, A.T.; Hlatini, V.A.; Thomas, R.S.; Chimonyo, M. A Review of the Utility of Potato By-Products as a Feed Resource for Smallholder Pig Production. *Anim. Feed Sci. Technol.* **2017**, *227*, 107–117. [CrossRef]
25. Li, M.Y.; Hou, X.L.; Wang, F.; Tan, G.F.; Xu, Z.S.; Xiong, A.S. Advances in the Research of Celery, an Important Apiaceae Vegetable Crop. *Crit. Rev. Biotechnol.* **2018**, *38*, 172–183. [CrossRef]
26. Aşkın Uzel, R. Sustainable Green Technology for Adaptation of Circular Economy to Valorize Agri-Food Waste: Celery Root Peel as a Case Study. *Manag. Environ. Qual. Int. J.* **2023**, *34*, 1018–1034. [CrossRef]
27. Taranu, I.; Marin, D.E.; Manda, G.; Motiu, M.; Neagoie, I.; Tabuc, C.; Stancu, M.; Olteanu, M. Assessment of the potential of a boron–fructose additive in counteracting the toxic effect of Fusarium mycotoxins. *Br. J. Nutr.* **2011**, *106*, 398–407. [CrossRef]
28. ISO 16472:2006; Animal Feeding Stuffs—Determination of Amylase-Treated Neutral Detergent Fiber Content (aNDF). ISO: Geneva, Switzerland, 2006. Available online: <https://www.iso.org/standard/37898.html> (accessed on 15 July 2024).
29. ISO 13906:2008; Animal Feeding Stuffs—Determination of Acid Detergent Fiber (ADF) and Acid Detergent Lignin (ADL) CONTENTS. ISO: Geneva, Switzerland, 2008. Available online: <https://www.iso.org/standard/43032.html> (accessed on 15 July 2024).
30. Anzano, J.M.; Perise, E.; Belarra, M.A.; Castillo, J.R. Determination of Calcium and Copper in Feedstuffs by Atomic Absorption Spectrometry Following a Digestion Procedure with H<sub>2</sub>SO<sub>4</sub> + H<sub>2</sub>O<sub>2</sub>. *Microchem. J.* **1995**, *52*, 268–273. [CrossRef]
31. ISO 7485:2000; Animal Feeding Stuffs—Determination of Potassium and Sodium Contents—Methods Using Flame-Emission Spectrometry. ISO: Geneva, Switzerland, 2000. Available online: <https://www.iso.org/standard/32070.html> (accessed on 15 July 2024).
32. COMMISSION REGULATION (EC) No 152/2009 of 27 January 2009, Laying down the Methods of Sampling and Analysis for the Official Control of Feed. Available online: <https://eur-lex.europa.eu/legal-content/EN/TXT/HTML/?uri=CELEX:32009R0152> (accessed on 22 July 2024).
33. Filip, M.; Vlassa, M.; Coman, V.; Halmagyi, A. Simultaneous Determination of Glucose, Fructose, Sucrose and Sorbitol in the Leaf and Fruit Peel of Different Apple Cultivars by the HPLC-RI Optimized Method. *Food Chem.* **2016**, *199*, 653–659. [CrossRef]
34. Filip, M.; Moldovan, M.; Vlassa, M.; Sarosi, C.; Cojocaru, I. HPLC Determination of the Main Organic Acids in Teeth Bleaching Gels Prepared with the Natural Fruit Juices. *Rev. Chim.* **2016**, *67*, 2440–2445.
35. Filip, M.; Silaghi-Dumitrescu, L.; Prodan, D.; Codruța, S.; Moldovan, M.; Cojocaru, I. Analytical Approaches for Characterization of Teeth Whitening Gels Based on Natural Extracts. *Key Eng. Mater.* **2017**, *752* KEM, 24–28. [CrossRef]
36. Vlassa, M.; Filip, M.; Tăranu, I.; Marin, D.; Untea, A.E.; Ropotă, M.; Dragomir, C.; Sărăcilă, M. The Yeast Fermentation Effect on Content of Bioactive, Nutritional and Anti-Nutritional Factors in Rapeseed Meal. *Foods* **2022**, *11*, 2972. [CrossRef] [PubMed]
37. Zielińska, D.; Turemko, M. Electroactive Phenolic Contributors and Antioxidant Capacity of Flesh and Peel of 11 Apple Cultivars Measured by Cyclic Voltammetry and HPLC–DAD–MS/MS. *Antioxidants* **2020**, *9*, 1054. [CrossRef] [PubMed]
38. Duda-Chodak, A.; Tarko, T.; Tuszyński, T. Antioxidant Activity of Apples—An Impact of Maturity Stage and Fruit Part. *Acta Sci. Pol. Technol. Aliment.* **2011**, *10*, 443–454. [PubMed]
39. Re, R.; Pellegrini, N.; Proteggente, A.; Pannala, A.; Yang, M.; Rice-Evans, C. Antioxidant Activity Applying an Improved ABTS Radical Cation Decolorization Assay. *Free Radic. Biol. Med.* **1999**, *26*, 1231–1237. [CrossRef]
40. Boultif, A.; Louër, D. Powder Pattern Indexing with the Dichotomy Method. *J. Appl. Crystallogr.* **2004**, *37*, 724–731. [CrossRef]
41. Canteri, M.H.G.; Renard, C.M.G.C.; Le Bourvellec, C.; Bureau, S. ATR-FTIR Spectroscopy to Determine Cell Wall Composition: Application on a Large Diversity of Fruits and Vegetables. *Carbohydr. Polym.* **2019**, *212*, 186–196. [CrossRef]
42. Hong, T.; Yin, J.Y.; Nie, S.P.; Xie, M.Y. Applications of Infrared Spectroscopy in Polysaccharide Structural Analysis: Progress, Challenge and Perspective. *Food Chem. X* **2021**, *12*, 100168. [CrossRef]

43. Kamnev, A.A.; Colina, M.; Rodriguez, J.; Ptitchkina, N.M.; Ignatov, V.V. Comparative Spectroscopic Characterization of Different Pectins and Their Sources. *Food Hydrocoll.* **1998**, *12*, 263–271. [[CrossRef](#)]
44. Liang, S.; McDonald, A.G. Chemical and Thermal Characterization of Potato Peel Waste and Its Fermentation Residue as Potential Resources for Biofuel and Bioproducts Production. *J. Agric. Food Chem.* **2014**, *62*, 8421–8429. [[CrossRef](#)]
45. Muhammad, K.; Nur, N.I.; Gannasin, S.P.; Adzahan, N.M.; Bakar, J. High Methoxyl Pectin from Dragon Fruit (*Hylocereus polyrhizus*) Peel. *Food Hydrocoll.* **2014**, *42*, 289–297. [[CrossRef](#)]
46. Zlatanović, S.; Ostojić, S.; Micić, D.; Rankov, S.; Dodevska, M.; Vukosavljević, P.; Gorjanović, S. Thermal Behaviour and Degradation Kinetics of Apple Pomace Flours. *Thermochim. Acta* **2019**, *673*, 17–25. [[CrossRef](#)]
47. Fan, M.; Dai, D.; Huang, B. Fourier Transform Infrared Spectroscopy for Natural Fibres. In *Fourier Transform*; Salih, S.M., Ed.; IntechOpen: Rijeka, Croatia, 2012.
48. Šoštarić, T.; Simić, M.; Lopičić, Z.; Zlatanović, S.; Pastor, F.; Antanasković, A.; Gorjanović, S. Food Waste (Beetroot and Apple Pomace) as Sorbent for Lead from Aqueous Solutions—Alternative to Landfill Disposal. *Processes* **2023**, *11*, 1343. [[CrossRef](#)]
49. Singh, L.; Kaur, S.; Aggarwal, P.; Kaur, N. Characterisation of Industrial Potato Waste for Suitability in Food Applications. *Int. J. Food Sci. Technol.* **2023**, *58*, 2686–2694. [[CrossRef](#)]
50. Boadi, N.O.; Badu, M.; Kortei, N.K.; Saah, S.A.; Annor, B.; Mensah, M.B.; Okyere, H.; Fiebor, A. Nutritional Composition and Antioxidant Properties of Three Varieties of Carrot (*Daucus carota*). *Sci. Afr.* **2021**, *12*, e00801. [[CrossRef](#)]
51. Hussain, S.; Jōudu, I.; Bhat, R. Dietary Fiber from Underutilized Plant Resources—A Positive Approach for Valorization of Fruit and Vegetable Wastes. *Sustainability* **2020**, *12*, 5401. [[CrossRef](#)]
52. Taranu, I.; Filip, M.; Vlassa, M.C.; Marin, D.; Untea, A.; Oancea, A.; Pertea, A.M. Assessing Comparatively The Bioactive Compounds Composition Of Apple Pomace Obtained From Three Apple Cultivars After Juice Extraction. *Anim. Food Sci. J. Iasi* **2023**, *80*, 29–38.
53. Luca, M.I.; Ungureanu-Iuga, M.; Mironeasa, S. Carrot Pomace Characterization for Application in Cereal-Based Products. *Appl. Sci.* **2022**, *12*, 7989. [[CrossRef](#)]
54. Rupérez, P.; Toledano, G. Celery By-Products as a Source of Mannitol. *Eur. Food Res. Technol.* **2003**, *216*, 224–226. [[CrossRef](#)]
55. Bouhlali, E.d.T.; Derouich, M.; Meziani, R.; Bourkhis, B.; Filali-Zegzouti, Y.; Alem, C. Nutritional, Mineral and Organic Acid Composition of Syrups Produced from Six Moroccan Date Fruit (*Phoenix dactylifera* L.) Varieties. *J. Food Compos. Anal.* **2020**, *93*, 103591. [[CrossRef](#)]
56. Javed, A.; Ahmad, A.; Tahir, A.; Shabbir, U.; Nouman, M.; Hameed, A. Potato Peel Waste—Its Nutraceutical, Industrial and Biotechnological Applications. *AIMS Agric. Food* **2019**, *4*, 807–823. [[CrossRef](#)]
57. Abdo, E.M.; Allam, M.G.; Gomaa, M.A.E.; Shaltout, O.E.; Mansour, H.M.M. Valorization of Whey Proteins and Beetroot Peels to Develop a Functional Beverage High in Proteins and Antioxidants. *Front. Nutr.* **2022**, *9*, 984891. [[CrossRef](#)] [[PubMed](#)]
58. Pistol, G.C.; Pertea, A.M.; Taranu, I. The Use of Fruit and Vegetable By-Products as Enhancers of Health Status of Piglets after Weaning: The Role of Bioactive Compounds from Apple and Carrot Industrial Wastes. *Vet. Sci.* **2024**, *11*, 15. [[CrossRef](#)] [[PubMed](#)]
59. Nićetin, M.; Pezo, L.; Pergal, M.; Lončar, B.; Filipović, V.; Knežević, V.; Demir, H.; Filipović, J.; Manojlović, D. Celery Root Phenols Content, Antioxidant Capacities and Their Correlations after Osmotic Dehydration in Molasses. *Foods* **2022**, *11*, 1945. [[CrossRef](#)] [[PubMed](#)]
60. Priečina, L.; Karklina, D. Natural Antioxidant Changes in Fresh and Dried Spices and Vegetables. *Int. J. Biol. Biomol. Agric. Food Biotechnol. Eng.* **2014**, *8*, 492–496.
61. Golubkina, N.A.; Kharchenko, V.A.; Moldovan, A.I.; Sekara, A.; Tallarita, A.; Caruso, G. Yield, Growth, Quality, Biochemical Characteristics and Elemental Composition of Plant Parts of Celery Leafy, Stalk and Root Types Grown in the Northern Hemisphere. *Plants* **2020**, *9*, 484. [[CrossRef](#)]
62. Lončarić, A.; Matanović, K.; Ferrer, P.; Kovač, T.; Šarkanj, B.; Babojelić, M.S.; Lores, M. Peel of Traditional Apple Varieties as a Great Source of Bioactive Compounds: Extraction by Micro-Matrix Solid-Phase Dispersion. *Foods* **2020**, *9*, 80. [[CrossRef](#)]
63. Ru, W.; Pang, Y.; Gan, Y.; Liu, Q.; Bao, J. Phenolic Compounds and Antioxidant Activities of Potato Cultivars with White, Yellow, Red and Purple Flesh. *Antioxidants* **2019**, *8*, 419. [[CrossRef](#)]
64. Sawicki, T.; Bączek, N.; Wiczkowski, W. Betalain Profile, Content and Antioxidant Capacity of Red Beetroot Dependent on the Genotype and Root Part. *J. Funct. Foods* **2016**, *27*, 249–261. [[CrossRef](#)]
65. Lau, W.K.; Van Chuyen, H.; Vuong, Q.V. Physical Properties, Carotenoids and Antioxidant Capacity of Carrot (*Daucus carota* L.) Peel as Influenced by Different Drying Treatments. *Int. J. Food Eng.* **2018**, *14*, 20170042. [[CrossRef](#)]
66. Drogoudi, P.D.; Michailidis, Z.; Pantelidis, G. Peel and Flesh Antioxidant Content and Harvest Quality Characteristics of Seven Apple Cultivars. *Sci. Hortic.* **2008**, *115*, 149–153. [[CrossRef](#)]
67. Sehm, J.; Lindermayer, H.; Dummer, C.; Treutter, D.; Pfaffl, M.W. The influence of polyphenol rich apple pomace or red-wine pomace diet on the gut morphology in weaning piglets. *J. Anim. Physiol. Anim. Nutr.* **2007**, *91*, 289–296. [[CrossRef](#)] [[PubMed](#)]
68. Guerrero, M.R.B.; Marques Da Silva Paula, M.; Zaragoza, M.M.; Gutiérrez, J.S.; Velderrain, V.G.; Ortiz, A.L.; Collins-Martínez, V. Thermogravimetric Study on the Pyrolysis Kinetics of Apple Pomace as Waste Biomass. *Int. J. Hydrogen Energy* **2014**, *39*, 16619–16627. [[CrossRef](#)]
69. Gowman, A.C.; Picard, M.C.; Rodriguez-Urbe, A.; Misra, M.; Khalil, H.; Thimmanagari, M.; Mohanty, A.K. Physicochemical Analysis of Apple and Grape Pomaces. *BioResources* **2019**, *14*, 3210–3230. [[CrossRef](#)]

70. Munir, S.; Daood, S.S.; Nimmo, W.; Cunliffe, A.M.; Gibbs, B.M. Thermal Analysis and Devolatilization Kinetics of Cotton Stalk, Sugar Cane Bagasse and Shea Meal under Nitrogen and Air Atmospheres. *Bioresour. Technol.* **2009**, *100*, 1413–1418. [[CrossRef](#)]
71. Elkhalfa, S.; Parthasarathy, P.; Mackey, H.R.; Al-Ansari, T.; Elhassan, O.; Mansour, S.; McKay, G. Biochar Development from Thermal TGA Studies of Individual Food Waste Vegetables and Their Blended Systems. *Biomass Conv. Bioref.* **2022**. [[CrossRef](#)]
72. Khosrowshahi, M.S.; Mashhadimoslem, H.; Emrooz, H.B.M.; Ghaemi, A.; Hosseini, M.S. Green Self-Activating Synthesis System for Porous Carbons: Celery Biomass Wastes as a Typical Case for CO<sub>2</sub> Uptake with Kinetic, Equilibrium and Thermodynamic Studies. *Diam. Relat. Mater.* **2022**, *127*, 109204. [[CrossRef](#)]
73. Mujtaba, G.; Hayat, R.; Hussain, Q.; Ahmed, M. Physio-chemical Characterization of Biochar, Compost and Co-composted Biochar Derived from Green Waste. *Sustainability* **2021**, *13*, 4628. [[CrossRef](#)]
74. Anukriti; Singh, N.; Upadhyay, D. XRD and SEM, ED Analysis of Solar Dried Vegetables. *Asian Food Sci. J.* **2022**, *21*, 25–37. [[CrossRef](#)]
75. Yi, S.; Lv, K.; Zhang, S.; Wang, W.; Li, X.; Li, J. Gel Quality and in Vitro Digestion Characteristics of Celery Nemipterus Virgatus Fish Sausages. *IOP Conf. Ser. Earth Environ. Sci.* **2020**, *512*, 012074. [[CrossRef](#)]
76. Imaizumi, T.; Szymańska-Chargot, M.; Pieczywek, P.M.; Chylińska, M.; Koziół, A.; Ganczarenko, D.; Tanaka, F.; Uchino, T.; Zdunek, A. Evaluation of Pectin Nanostructure by Atomic Force Microscopy in Blanched Carrot. *LWT* **2017**, *84*, 658–667. [[CrossRef](#)]

**Disclaimer/Publisher's Note:** The statements, opinions and data contained in all publications are solely those of the individual author(s) and contributor(s) and not of MDPI and/or the editor(s). MDPI and/or the editor(s) disclaim responsibility for any injury to people or property resulting from any ideas, methods, instructions or products referred to in the content.